

Strong Gravitational Lensing and Localization of Merging Massive Black Hole Binaries with LISA

Naoki Seto

Theoretical Astrophysics, MC 130-33, California Institute of Technology, Pasadena, CA 91125

We study how the angular resolution of LISA for merging massive black-hole binaries would be improved if we could observe multiple “images” (gravitational waves) due to strong gravitational lensing. As the correlation between fitting parameters is reduced by additional information of the second image, the error box in the sky could be significantly reduced. This improvement would be very helpful to specify the host galaxy of a binary. Angular resolution expected with multiple detectors is also discussed.

I. INTRODUCTION

Black holes are a very fascinating prediction of general relativity. Recent observations indicate that massive black holes (MBHs) exist at the centers of many galaxies and their masses have strong correlation with properties of their host galaxies [1]. Binary MBHs would be formed by merging of galaxies that harbor MBHs [2]. Coalescence of such binary is the most energetic event in the Universe. It finally releases enormous energy (several orders smaller than $c^5/G \sim 4 \times 10^{59}$ erg/sec) in characteristic time scale $GM/c^3 \sim 5(M/10^6 M_\odot)$ sec (M : mass of the system). The Laser Interferometer Space Antenna (LISA) can observe gravitational waves from MBH binaries with high signal to noise ratio (SNR) [3]. In the case of equal mass binaries the expected SNR at a given distance would be maximum around redshifted masses $\sim 10^6 M_\odot$ and becomes $\gtrsim 10^3$ even at cosmological distances [4]. By fitting gravitational wave from a MBH binary with templates prepared in advance we can make stringent test of general relativity and obtain various important information of black holes (*e.g.* mass, spin). Therefore gravitational waves from MBH binaries are, by themselves, very interesting signal for relativistic astrophysics [3, 5].

If we can identify their host galaxies, it would also bring significant impacts on astrophysics and cosmology. By detailed follow-up observation using electro-magnetic waves at various frequency bands we might discover absorbing properties of the galaxies or obtain fundamental clues to elucidate evolution of MBHs. Angular direction of coalescing MBH binaries could be, in principle, estimated by analyzing data of LISA. Due to annual revolution and rotation of LISA the signal from a MBH binary shows modulation that depends strongly on the sky position of the binary. For equal mass MBH binaries at $z \sim 1$ the angular resolution of LISA would be typically $\sim 10^{-4}$ sr for redshifted masses $\sim 10^6 M_\odot$ [4]. The resolution becomes worth for high redshift MBH binaries. The number of bright galaxies would be $\sim 10^4$ in one square degree ($\sim 3 \times 10^{-4}$ sr), and the angular resolution of LISA is not sufficient to fully specify the host galaxy of a cosmological MBH binary [4]. Thus improvement of the angular resolution for a MBH binary would be crucially helpful to select candidates for its host galaxy using electro-magnetic telescopes. Possible mechanisms for this improvement is worth explored.

In this context it has been discussed that higher harmonics of gravitational waves [6], precession of orbital plane of rapidly spinning system [7], or effects caused by finite arm-length of LISA [8] could become important in some situations. In this paper we show that the angular resolution for a MBH binary could be significantly improved, if we could observe multiple “images” of gravitational wave caused by strong gravitational lensing. Our point is not the amplification of the signal but observation of a same source at different epochs. The intrinsic binary parameters such as the chirp mass can be determined very accurately from gravitational waves. Then it would not be a hard task to pair two lensed signals from a merging MBH binary.

If we assume that MBH binaries would coalesce shortly (less than the Hubble time) after merging of their host galaxies, hierarchical model of structure formation suggests that coalescence rate of MBH binaries could be up to $\sim 100 \text{yr}^{-1}$, and its distribution might be much higher at high redshift than low redshift $z \lesssim 1$ [9]. Probability τ of the strong gravitational lensing also depends strongly on the redshift of the source. At $z \sim 1$ we have the probability of only $\tau \lesssim 10^{-3}$, but the it could reach several percent at $z \sim 5$ [10]. Thus we might obtain multiple images (more preciously the chirping gravitational waves) of distant MBH binaries. In this paper it is shown that the additional images caused by lensing with time delay $\Delta T \gtrsim 0.1$ yr would largely decrease the correlations between fitting parameters of the templates, and the angular resolution of a MBH binary could be dramatically improved.

This paper is organized as follows. In Sec II we briefly discuss signal analysis for a single image (IIA) and for multiple images (IIB). Various numerical results are presented in Sec III. We also give the angular resolution obtained with multiple detectors that are widely separated (IIIC). Our study is summarized in Sec IV.

II. ANALYSIS

A. observation of a chirping gravitational wave

Three spacecrafts of LISA keep a nearly equilateral triangle configuration and move annually around the Sun with changing the orientation of the triangle. As discussed below, direction of a gravitational wave source can be estimated from the wave signal affected by (i) the Doppler effect due to the revolution of the detectors around the Sun and (ii) the amplitude modulation due to the rotation of the triangle and the increase of the wave frequency (chirp signal) [3, 4]. For response of LISA to gravitational waves we follow [11] for the time-delay interferometry (TDI) analysis that cancels the laser frequency fluctuations of data streams [12].

We name three spacecrafts as 1, 2, and 3 and use notation L_i ($i = 1, 2, 3$) to denote the arm-length opposite to the spacecraft i . Information of binaries is extracted by using three data streams $A(t)$, $E(t)$ and $T(t)$ that form orthogonal basis for the laser-noise canceling combinations. These three data A , E and T are made from six (one-way) relative frequency fluctuations $y_{ij}(t)$ ($i, j = 1, 2, 3, i \neq j$) at different times (see [11] for explicit expressions of A , E , T in terms of $y_{ij}(t)$). The signal y_{ij} is measured at spacecraft j with transmission from spacecraft k ($\neq i, \neq j$) along the arm L_i .

Our analysis is similar to [4] (see also [13, 14, 15]). But as in [8] we do not use the long wave approximation that is valid for incoming gravitational waves larger than the arm-length of LISA $L = 5.0 \times 10^6$ km, corresponding to $f = c/2\pi L \sim 0.01$ Hz. The study in [8] is somewhat incomplete, as the TDI analysis was not included properly. This point is also remediated in this paper. For simplicities we assume that the arm-lengths L_i are equal.

First we briefly discuss the gravitational waveform from a MBH binary with circular orbit. In this paper we only include the inspiral waveforms. For larger MBH binaries the contribution of ring-down could be important for SNR [14]. We use the stationary phase approximation and the restricted post-Newtonian approach with 1.5-PN phase [16] that is given in Fourier space as follows

$$\Psi(f) = 2\pi f t_c - \phi_c - \frac{\pi}{4} + \frac{3}{4} (8\pi G c^{-3} \mathcal{M}_z f)^{-5/3} \left[1 + \frac{20}{9} \left(\frac{943}{336} + \frac{11\mu_z}{4M_z} \right) x + (4\beta - 16\pi) x^{3/2} \right], \quad (2.1)$$

where t_c and ϕ_c are integration constants, and the former contains information of the coalescence time measured at the Sun not at the detector. The difference between them is included in eq.(2.3). β is the spin-orbit coupling coefficient (we put its true value $\beta = 0$). μ_z , M_z \mathcal{M}_z are the reduced mass, the total mass, the chirp mass respectively. All of the mass parameters are multiplied by the factor $(1+z)$ (z : redshift of the binary) with the suffix z . The total mass M_z is given by other two masses as $M_z = \mathcal{M}_z^{5/2} \mu_z^{-3/2}$. The post-Newtonian expansion parameter $x = O(v^2/c^2)$ is defined as $x \equiv \{G\pi c^{-3} M_z f\}^{2/3}$.

For simplicities we first consider gravitational waves propagating in a homogeneous background. Effects of lensing would be discussed later. The incoming gravitational wave from a binary is decomposed into plus and cross polarization modes. It is convenient to use the principle axes (\mathbf{p}, \mathbf{q}) defined by the direction $\boldsymbol{\Omega}_s$ and orientation $\boldsymbol{\Omega}_l$ of the binary as $\mathbf{p} = \boldsymbol{\Omega}_s \times \boldsymbol{\Omega}_l / |\boldsymbol{\Omega}_s \times \boldsymbol{\Omega}_l|$ and $\mathbf{q} = -\boldsymbol{\Omega}_s \times \mathbf{p}$. The plus mode has the polarization tensor $e_{ab}^+ = p_a p_b - q_a q_b$ and the cross has $e_{ab}^\times = p_a q_b + q_a p_b$. The relative frequency shift, for example, $y_{31}(t)$ due to these two modes is expressed as

$$y_{31}(t) = \frac{1}{2} (\pi f)^{2/3} (\cos 2\psi_{12} A_+ + i \sin 2\psi_{12} A_\times) (1 - \cos \theta_{12}) [U(t, 1) - U(t - \tau, 2)], \quad (2.2)$$

where τ is the time $\tau = L/c \sim 17$ sec and the function

$$U(t, j) = \exp[-2\pi i f(t + \mathbf{x}_j \cdot \boldsymbol{\Omega}_s / c)] \quad (2.3)$$

has information of the phase of the incoming wave at the detector j (with position \mathbf{x}_j measured from the Sun) and time t . In Eq.(2.2) we have neglected very small relative motions between the detectors in the time scale τ and also the time variation of the frequency in the time scale $1\text{AU}/c = 500$ sec. The coefficients A^+ and A^\times are given in terms of an amplitude A as $A^+ = A(1 + \cos^2 I)$ and $A^\times = 2A \cos I$ with cosine of the inclination angle $\cos I \equiv \boldsymbol{\Omega}_s \cdot \boldsymbol{\Omega}_l$. In Eq.(2.2) θ_{jk} is the angle between the direction of a binary $\boldsymbol{\Omega}_s$ and the arm $\mathbf{x}_j - \mathbf{x}_k$, and the the principle polarization angle ψ_{jk} is given by $\tan \psi_{jk} = [(\mathbf{x}_j - \mathbf{x}_k) \cdot \mathbf{q}] / [(\mathbf{x}_j - \mathbf{x}_k) \cdot \mathbf{p}]$. These two angles θ_{jk} and ψ_{jk} change with motion of spacecrafts.

The Doppler effects appear in the factor $U(t, j)$. The TDI data streams at time t are written by linear combinations of y_{ij} at different times, *e.g.* t , $t - \tau$ or $t - 2\tau$. Due to the finiteness of the arm-length, the response to gravitational waves shows complicated behavior that depends strongly on the angular position of a MBH binary. Effects of the finite arm-length on the estimation of the source direction could become important around $\sim 10^5 + 10^5 M_\odot$ in the case of equal mass binaries [8]. In the long wave limit $f\tau \ll 1$ the above expression (2.2) becomes simplified. The analysis by Cutler [4] is essentially using this limit, and the amplitude modulation and phase modulation by Doppler

effects can be analyzed separately. As a reference we also examine the angular resolution of MBH binaries with this method for response of LISA to gravitational waves.

For intrinsic detector's noise for measurement of the fluctuations y_{ij} there are two main elements relevant for the combinations A, E, T . They are the proof mass noise and the optical path noise. We use their spectra [12]

$$S_y^{proof-mass}(f) = 2.5 \times 10^{-48} \left(\frac{f}{1\text{Hz}} \right)^{-2} \text{Hz}^{-1}, \quad (2.4)$$

$$S_y^{optical-path}(f) = 1.8 \times 10^{-37} \left(\frac{f}{1\text{Hz}} \right)^2 \text{Hz}^{-1}. \quad (2.5)$$

It is a simple task to obtain the noise for the three combinations A, E, T . But note that the detector's noise below 0.1mHz is somewhat controversial (see *e.g.* [14, 17]). This frequency region strongly affects the results of larger MBH binaries.

We also include the Galactic binary confusion noise [18] using the following simple approximation

$$S_h^{Gc}(f) = \begin{cases} 4 \times 10^{-37} \left(\frac{f}{1\text{mHz}} \right)^{-7/3} \text{Hz}^{-1} & (f \leq 10^{-2.7}\text{Hz}) \\ 0 & (f > 10^{-2.7}\text{Hz}) \end{cases} \quad (2.6)$$

given for gravitational wave amplitude h for one year observation. This confusion noise is about 10 times larger (for h) than detector's noise at 1mHz (see figure 5 of [11]). For simplicities we neglect the anisotropies of the Galactic confusion noise in this paper.

We integrate each chirping gravitational wave for 1yr before the coalescence up to the cut-off frequency f_{max} when the binary separation becomes $r = 6GM_z/c^2(1+z)$, corresponding to

$$f_{max} = 0.04 \left(\frac{M_z}{10^5 M_\odot} \right)^{-1} \text{Hz}. \quad (2.7)$$

In contrast wave frequency f observed at T yr before the coalescence time t_c is roughly given by

$$f = 1.9 \times 10^{-4} \left(\frac{\mathcal{M}_z}{0.87 \times 10^5 M_\odot} \right)^{-5/8} \left(\frac{T}{1\text{yr}} \right)^{-3/8} \text{Hz}. \quad (2.8)$$

Signal to noise ratio SNR of detection is determined by the amplitudes of the modes A, E and T and the noise spectra $S_A(f), S_E(f)$ and $S_T(f)$ constructed from detector's noises (2.4) (2.5) and confusion noise (2.6). We calculate the signal to noise ratio of inspiral waves as follows [19, 20]

$$\text{SNR}^2 = 4 \sum_{B=A,E,T} \int_{f_1}^{f_{min}} \frac{B(f)B^*(f)}{S_B(f)} df, \quad (2.9)$$

where f_1 is the initial frequency for signal integration. In the present study the number of the fitting parameters $\{\alpha_i\}$ for each chirping gravitational wave is 10. They are $\{\alpha_i\} = \{\mathcal{M}_z, \mu_z, \beta, t_c, \phi_c, A, \theta_s, \phi_s, \theta_l, \phi_l\}$. Angular variables (θ_s, ϕ_s) represent the direction of the binary Ω_s in a fixed frame around the Sun, and (θ_l, ϕ_l) represent its orientation Ω_l . Variance of the parameter estimation errors $\Delta\alpha_i$ are evaluated by the Fisher information matrix Γ_{ij} as $\langle \Delta\alpha_i \Delta\alpha_j \rangle = \Gamma_{ij}^{-1}$ where Γ_{ij} is given as [20]

$$\Gamma_{ij} = 4 \sum_{B=A,E,T} \int_{f_1}^{f_{min}} \frac{\partial_i B(f) \partial_j B^*(f)}{S_B(f)} df. \quad (2.10)$$

Following Cutler [4] we use the notation $\Delta\Omega_s \equiv 2\pi \sin\theta_s \sqrt{\langle \Delta\theta_s^2 \rangle \langle \Delta\phi_s^2 \rangle - \langle \Delta\theta_s \Delta\phi_s \rangle^2}$ for the angular resolution of a binary in the sky.

Our results for the angular resolution $\Delta\Omega_s$ changes only slightly for masses $\gtrsim 10^4 M_\odot$ when we switch the integration time from 1yr to 10 yr. MBH binaries are put at $z = 3$ in a universe with background cosmological parameters $\Omega_0 = 0.3$, $\lambda_0 = 0.7$ (spatially flat universe) and $H_0 = 71\text{km/sec/Mpc}$. In this background model the luminosity distance d_L becomes $d_L = 25\text{Gpc}$ at $z = 3$ and $d_L = 6.5\text{Gpc}$ at $z = 1$.

B. analysis for multiple images by lensing

Now we discuss the parameter fitting for multiple images caused by strong gravitational lenses. As we show below improvement of the angular resolution $\Delta\Omega_s$ due to lensed multiple images could be very effective for time delay $\Delta T \gtrsim 0.1\text{yr}$. On the other hand time delay larger than the operation period of LISA (nominally ~ 3 yrs, but possibly ~ 10 yrs) is irrelevant for our analysis. Thus our main target is multiple images with time delay $0.1\text{yr} \lesssim \Delta T \lesssim 10\text{yr}$. LISA has good sensitivity to gravitational waves with frequency $10^{-4}\text{Hz} \lesssim f \lesssim 10^{-1}\text{Hz}$ that is much higher than the inverse of the relevant time delay $(\Delta T)^{-1} \lesssim 3 \times 10^{-7}\text{Hz}$. Note also that the latter is smaller than f given in eq.(2.8) with $T = 1\text{yr}$ and $\mathcal{M}_z \lesssim 10^8 M_\odot$. Therefore the geometric optics approximation is valid in our study and the structure of phase is not changed by the lensing [21, 22]. We take the same parameters $\mathcal{M}_z, \mu_z, \phi_c, \beta$ for the phases eq.(2.1) of all the multiple images from a source, but the coalescence time t_c is, of course, different. In some cases the substructure of lensing galaxy might complicate the problem [23].

In the case of homogeneous and isotropic universe the wave amplitude A is simply given in terms of the luminosity distance d_L and the chirp mass \mathcal{M}_z as [24]

$$A_0 = \frac{2G^{5/3}\mathcal{M}_z^{5/3}}{c^4 d_L}. \quad (2.11)$$

The above relation can be used to determine d_L from observed gravitational wave and also to specify the redshift of the binary z by inversion of the d_L - z relation if cosmological parameters are known accurately [14, 24]. Note that in general the chirp mass \mathcal{M}_z is determined more accurately than the amplitude A using time evolution of the phase.

For signals affected by strong lensing we fit different values A_i for the amplitudes of multiple images. We cannot apply the above inversion for estimation of z , but this damage is not serious for identifying high- z MBH binaries, considering the accumulated effects of weak lensing. At $z \sim 3$ the rms fluctuations of the amplification by weak lensing could become ~ 0.2 and hamper simple application of the above inversion even for a single image [15, 25].

Here we discuss fitting of the angular variables $(\theta_s, \phi_s, \theta_l, \phi_l)$. First we evaluate typical image separation for a lensed source. As a reference we use the singular isothermal sphere approximation for the density profile of lensing galaxy. In this model we have the following explicit relation for the image separation angle θ and the time delay ΔT [26]

$$\Delta T = \frac{\theta^2}{2c} \frac{D_{OL} D_{OS}}{D_{LS}} (1 + z_L) y = 1.3 \left(\frac{\theta}{5''} \right)^2 \left(\frac{D_{OL}}{D_{LS}} \right) \left(\frac{D_{OS}}{1.4\text{Gpc}} \right) \left(\frac{1 + z_L}{2} \right) \left(\frac{y}{0.5} \right) \text{yr}, \quad (2.12)$$

where $D = d_L/(1 + z)^2$ is the angular diameter distance (*e.g.* D_{OL} : between the observer and the lens), z_L is the redshift of the lens, y is the normalized impact parameter with $y < 1$ for occurrence of multiple images in the case of the isothermal sphere approximation. The image separation ($\lesssim 5''$) for relevant time delay $\Delta T \sim 1\text{yr}$ is much smaller than the angular resolution of the source direction for cosmological MBH binaries, as confirmed later. This means that we can use the same fitting parameters (θ_s, ϕ_s) for the direction of the binary.

Polarization tensor \mathbf{e}_{ab} for gravitational wave is parallelly transported along a null geodesic [27]. We can easily confirm that the directions of tetrad vectors along with the lensed null geodesics change only order of the image separation that is generally much smaller than the resolution of the orientation of a cosmological MBH binary (θ_l, ϕ_l) . These means that polarization properties of the multiple images can not be distinguished observationally and a same fitting parameter (θ_l, ϕ_l) can be also used for the orientation of multiple images.

Let us briefly summarize number of the fitting parameters. For n -multiple images from a same source we can take eight common parameters $\{\mathcal{M}_z, \mu_z, \beta, \phi_c, \theta_s, \phi_s, \theta_l, \phi_l\}$, but fit different ones $\{A_i, t_{ci}\}$ for each image ($i = 1, \dots, n$). Thus the total number of the fitting parameters becomes $8 + 2n$. In the following analysis we fix the true value of the each wave amplitude A (both un-lensed and lensed) by $A = A_0$. This would give conservative results for magnitude of the parameter estimation errors in the case of lensed signals. With our setting SNR depends on the total number of images n as $\text{SNR} \propto n^{1/2}$.

III. ANGULAR RESOLUTIONS FOR MBH BINARIES

A. basic analysis

We calculate the parameter estimation errors with (i) the TDI method described in Sec II and (ii) the method by Cutler [4] that uses the long-wave approximation. Effective noise curves are somewhat different for these two. In this section various averaged quantities, such as SNR or the angular resolution $\Delta\Omega$, are evaluated by taking geometrical

averages for 100 MBH binaries at $z = 3$ with random directions (θ_s, ϕ_s) and orientations (θ_l, ϕ_l) . For simplicities we only study equal mass binaries. The time delay is fixed at $\Delta T = 1/3\text{yr}$ unless otherwise stated.

In Figure 1 the averaged SNR is presented for redshifted masses $4 \times 10^3 - 4 \times 10^8 M_\odot$ (true masses $10^3 - 10^8 M_\odot$). Hereafter we mainly use the redshifted mass $m_z = m_{1z} = m_{2z}$ to show the mass dependence. When we decrease the mass from $m_z \sim 10^8 M_\odot$, SNR becomes large around $m_z \sim 10^6 M_\odot$. This is because the binary confusion noise disappear around $f \sim 10^{-2.7}\text{Hz}$ in our models and this frequency corresponds to the coalescence frequency f_{\max} of MBH binary with mass $m_z \sim 10^6 M_\odot$ as in eq.(2.7). SNR for lensed two images simply increases a factor of $\sim 1.5 \sim \sqrt{2}$ as easily expected.

In Figure 2 we show the averaged angular resolution as a function of redshifted mass m_z . For single images the averaged resolution $\Delta\Omega_1$ shows weak dependence on the mass for the TDI method, and nearly constant $\sim 2 \times 10^{-3}\text{sr}$ for MBH binaries with masses from $m_z \sim 10^5 M_\odot$ to $10^8 M_\odot$ at $z = 3$. This is a remarkable contrast with Figure 1 for SNR that shows a steep rise around $m_z \sim 10^5 - 10^6 M_\odot$. Using the simple method by Cutler we find that the sky positions of MBH binaries with $m_z \gtrsim 10^5 M_\odot$ are mainly estimated by the amplitude modulation due to rotation of the Detectors. The Doppler phase modulation shows contribution at $m_z \lesssim 10^5 M_\odot$.

When the second image is added by time delay of lensing, situations change drastically. The angular resolution $\Delta\Omega_2$ obtained for two images with $m_z \sim 4 \times 10^5 M_\odot$ would improved more than two order of magnitude, comparing with the single image $\Delta\Omega_1$. The ratio $\Delta\Omega_1/\Delta\Omega_2$ decreases at both smaller and larger masses. It becomes ~ 10 at $m_z \sim 10^4 M_\odot$ and ~ 5 at $m_z \sim 10^8 M_\odot$. This mass dependence is discussed later. We also found that the errors for the intrinsic binary parameters such as the chirp mass would be changed only factor ~ 2 or so by the second image.

In Figure 3 we show the histograms of the angular resolutions $\Delta\Omega_1$ and $\Delta\Omega_2$ for our 100 realizations of MBH binaries with redshifted masses $m_z = 4 \times 10^3 M_\odot, 4 \times 10^5 M_\odot$ and $4 \times 10^7 M_\odot$. Impacts of the lensing are also apparent with these figures.

So far we have fixed the time delay at $\Delta T = 1/3\text{yr}$. In Figure 4 we present the ratio $\Delta\Omega_1/\Delta\Omega_2$ as a function of the time delay ΔT . Due to the periodicity of the configuration of LISA the results obtained for $\Delta T\text{yr}$ are same as $\Delta T + N\text{yr}$ with an integer N . As our results are given in the form of ratio $\Delta\Omega_1/\Delta\Omega_2$, they do not depend on the distance or redshift to the source as long as we use the redshifted masses. The factors $\Delta\Omega_1/\Delta\Omega_2$ depend only weakly on the time delay with $\Delta T \gtrsim 0.1\text{yr}$.

B. third image

We have also calculated the angular resolution $\Delta\Omega_3$ in the case that we could observe totally three images. We set the two time delays measured from the first images as $\Delta T = 1/3\text{ yr}$ and $\Delta T = 2/3\text{ yr}$, and fixed the amplitudes of three images by A_0 given in eq.(2.11). The ratios $\Delta\Omega_1/\Delta\Omega_3$ become ~ 40 ($m_z = 4 \times 10^3 M_\odot$), ~ 800 ($4 \times 10^5 M_\odot$) and ~ 22 ($4 \times 10^7 M_\odot$). For the first two images analyzed in the previous subsection the ratios $\Delta\Omega_1/\Delta\Omega_2$ are ~ 13 ($4 \times 10^3 M_\odot$), ~ 300 ($4 \times 10^5 M_\odot$) and ~ 9 ($4 \times 10^7 M_\odot$). Therefore the effects of the third images are not so drastic as the second ones.

C. multiple detectors

We have shown that observation of multiple images due to lensing could significantly improve the angular resolution $\Delta\Omega$. But we cannot bet this passive effect for most merging MBH binaries, considering the probability. In usual situation we could only detect a single image. Using multiple detectors is one positive method to improve the resolution. In this case we can take the same fitting parameters also for the amplitude A and the coalescence time t_c (at the Sun). The former is important as the amplitude A and the angular variables would correlate strongly (see eq.(2.2)). The latter means that we can take advantage of the time delay between detectors that are closely related to the direction of a binary.

As a simple extension of our analysis for lensing, we calculate the angular resolution $\Delta\Omega_{II}$ with two detectors that has the same specification with LISA. Two detectors are on the Earth orbit around the Sun as in LISA, but we put forward one to another with angle $2\pi/3$ corresponding to $1/3\text{yr}$ for orbital time. Thus their distance is fixed at $1\text{AU} \times 2 \times \sin(\pi/3) = 1.73\text{AU}$, and their orientations are always different from each other. For simplicities we assume that noises of the data streams measured by two detectors are independent. This would be a valid approximation for detectors' noise, but might not be for the binary confusion noise.

The ratio of angular resolutions for a single LISA $\Delta\Omega_1$ and for two LISAs $\Delta\Omega_{II}$ becomes $\Delta\Omega_1/\Delta\Omega_{II} \sim 10^2$ ($4 \times 10^3 M_\odot$), $\sim 6 \times 10^3$ ($4 \times 10^5 M_\odot$) and ~ 30 ($4 \times 10^7 M_\odot$). Therefore even for binaries at $z = 3$ the angular position of a merging MBH binary can determined with error box $\sim 10^{-6}\text{sr}$, namely (several minutes) 2 . This area in the celestial sphere is close to the resolution of Gamma-Ray-Bursts to determine their host galaxies. When another

detector (totally three) is added with position characterized by 1/3yr and 2/3yr, the ratio $\Delta\Omega_1/\Delta\Omega_{III}$ becomes ~ 400 , $\sim 4 \times 10^4$ and ~ 60 respectively.

D. effective time

As shown above, the angular resolution $\Delta\Omega$ could be improved significantly around $m_z = 10^5 \sim 10^6 M_\odot$. Here we analyze this mass dependence. Roughly speaking, SNR characterizes the magnitude of the Fisher matrix Γ_{ij} as we can understand from eqs.(2.9) and (2.10). When correlation (degeneracy) between the fitting parameters is large, the parameter estimation errors such as $\Delta\Omega$ become also large. This correlation depends strongly on the configuration of LISA around the epoch when SNR accumulates. In this situation an independent information *e.g.* added by the second image, has important role to reduce the correlation and improve the angular resolution $\Delta\Omega$. This fact can be anticipated by comparing Figures 1 and 2.

The angular directions of MBH binaries are mainly estimated from the amplitude modulation and the Doppler phase modulation by revolution and rotation of LISA. A long term observation is crucial to determine them well. Therefore correlation between parameters including the direction would be related to the effective observational period, and a binary with a shorter observational period could have larger ratio $\Delta\Omega_1/\Delta\Omega_2$. Let us define a time t_{eff} by weighting the time before coalescence $t_c - t$ with amplitude of the wave $h(f)$ and the noise curve $S_h(f)$ as follows

$$t_{\text{eff}}^2 \equiv \frac{\left(4 \int \frac{h(f)h^*(f)(t-t_c)^2}{S_h(f)} df \right)}{\left(4 \int \frac{h(f)h^*(f)}{S_h(f)} df \right)}. \quad (3.1)$$

Here we formally wrote down the above expression (see eq.(2.9)). The denominator is nothing but the square of SNR. As the weight factor $|h(f)|/S_h(f)^{1/2}$ does not have a very spiky structure, we can regard t_{eff} as an effective observational period of binaries. For monochromatic sources we have $t_{\text{eff}} = 1/\sqrt{3}$ yr. In figure 5 we show the time t_{eff} (solid curve) and the ratio of the angular resolution $\Delta\Omega_2/\Delta\Omega_1$ (dashed curve). The overall shape of them are similar as expected.

The mass dependence of t_{eff} could be understood as follows. For a larger mass binaries with $\gtrsim 10^5 M_\odot$, SNR (denominator of eq.(3.1)) mainly comes from wave close the final coalescence. But these waves have small contribution to the numerator. The binary with mass $m_z \lesssim 10^6 M_\odot$ has coalescence frequency larger than $10^{-2.7}$ Hz that is critical for the Galactic binary confusion noise. Therefore effective observational time t_{eff} decrease significantly around $m_z \lesssim 10^6 M_\odot$. A smaller mass ($m_z \lesssim 10^4 M_\odot$) binaries have longer time to stay in the sensitive frequency region, and the effective time t_{eff} increases.

IV. SUMMARY

In this paper we have studied how the angular resolution of LISA would be improved if we can observe multiple images due to strong gravitational lensing. It is found that the error box in the sky could be typically 100 times smaller for redshifted mass $m_z = 10^5 \sim 10^6 M_\odot$. The improvement of the angular resolution depends strongly on the masses of MBH binaries. This mass dependence can be roughly explained with using effective observational time for a binary.

We have mainly discussed the effects of lensing on the Matched filtering analysis of gravitational waves, but lensing would be also of great advantages to search the host galaxy of MBH binary using electro-magnetic waves. Beside the fact itself that the target is lensed, additional information obtained from gravitational waves, such as the time delay or ratio of the amplification factors of images, would be used to specify the host galaxy.

We have also calculated the angular resolution expected for multiple detectors and found that the resolution could be improved by factor of $\sim 6 \times 10^3$ ($m_z \sim 4 \times 10^5 M_\odot$) comparing with a single detector. If LISA could detect gravitational waves from MBH binaries, very exciting results might be obtained by launching another detector.

Acknowledgments

The author would like to thank R. Takahashi for valuable discussions. He also thanks S. Larson and A. Cooray for helpful comments.

[1] D. Merritt and L. Ferrarese, arXiv:astro-ph/0107134.

[2] M. C. Begelman, R. D. Blandford, and M. J. Rees, *Nature* **287**, 307 (1980).

[3] P. L. Bender *et al.*, *LISA Pre-Phase A Report*, Second edition, July 1998.

[4] C. Cutler, *Phys. Rev. D* **57**, 7089 (1998).

[5] C. Cutler and K. S. Thorne, arXiv:gr-qc/0204090.

[6] T. A. Moore and R. W. Hellings, *Phys. Rev. D* **65**, 062001 (2002) [arXiv:gr-qc/9910116]; A. M. Sintes and A. Vecchio, in *Gravitational Waves – Third Amaldi Conference*, Ed. S. Meshkov (American Institute of Physics), pp. 403-404 (2000).

[7] A. Vecchio, arXiv:astro-ph/0304051.

[8] N. Seto, *Phys. Rev. D* **66**, 122001 (2002) [arXiv:gr-qc/0210028].

[9] M. G. Haehnelt, *Mon. Not. Roy. Astron. Soc.* **269**, 199 (1994); K. Menou, Z. Haiman and V. K. Narayan, *Astrophys. J.* **558**, 535 (2001); A. H. Jaffe and D. C. Backer, *Astrophys. J.* **583**, 616 (2003); J. S. Wyithe and A. Loeb, arXiv:astro-ph/0211556.

[10] D. E. Holz, M. C. Miller and J. M. Quashnock, arXiv:astro-ph/9804271.

[11] T. A. Prince, M. Tinto, S. L. Larson and J. W. Armstrong, *Phys. Rev. D* **66**, 122002 (2002) [arXiv:gr-qc/0209039].

[12] M. Tinto and J. W. Armstrong, *Phys. Rev. D* **59**, 102003 (1999); J. W. Armstrong, F. B. Estabrook and M. Tinto, *Astrophys. J.* **527**, 814 (1999); J. W. Armstrong, F. B. Estabrook and M. Tinto, *Class. Quant. Grav.* **18**, 4059 (2001); R. W. Hellings, *Phys. Rev. D* **64**, 022002 (2001); S. V. Dhurandhar, K. R. Nayak and J. Y. Vinet, *Phys. Rev. D* **65**, 102002 (2002).

[13] A. Vecchio and C. Cutler, in *Laser Interferometer Space Antenna*, ed. W. M. Falkner (AIP Conference Proceedings 456), pp. 101-109 (1998).

[14] S. A. Hughes, *Mon. Not. Roy. Astron. Soc.* **331**, 805 (2002) [arXiv:astro-ph/0108483].

[15] D. E. Holz and S. A. Hughes, arXiv:astro-ph/0212218.

[16] C. Cutler *et al.*, *Phys. Rev. Lett.* **70**, 2984 (1993) [arXiv:astro-ph/9208005].

[17] P. L. Bender, *Class. Quant. Grav.* **20**, S301 (2003).

[18] P. L. Bender and D. Hils, *Class. Quant. Grav.* **14**, 1439 (1997); N. J. Cornish and S. Larson, *Class. Quant. Grav.* **20**, S163 (2003) [arXiv:gr-qc/0206017]; A. J. Farmer and E. S. Phinney, arXiv:astro-ph/0304393.

[19] K. S. Thorne, in *300 Years of Gravitation*, edited by S. W. Hawking and W. Israel (Cambridge, England, 1987), pp.330-458.

[20] L. S. Finn, *Phys. Rev. D* **46**, 5236 (1992) [arXiv:gr-qc/9209010]; C. Cutler and E. E. Flanagan, *Phys. Rev. D* **49**, 2658 (1994) [arXiv:gr-qc/9402014].

[21] T. T. Nakamura, *Phys. Rev. Lett.* **80**, 1138 (1998).

[22] R. Takahashi and T. Nakamura, arXiv:astro-ph/0305055.

[23] S. Mao and P. Schneider, *Mon. Not. Roy. Astron. Soc.* **295**, 587 (1998); M. Chiba, *Astrophys. J.* **565**, 17 (2001).

[24] B. F. Schutz, *Nature* **323** (1986) 310.

[25] A. J. Barber, P. A. Thomas, H. M. Couchman and C. J. Fluke, *Mon. Not. Roy. Astron. Soc.* **319**, 267 (2000);

[26] P. Schneider, J. Ehlers, and E. E. Falco, *Gravitational Lenses* (Springer-Verlag, Berlin,1992).

[27] C. W. Misner, K. S. Thorne and J. A. Wheeler, *Gravitation* (Freeman, San Francisco, 1973).

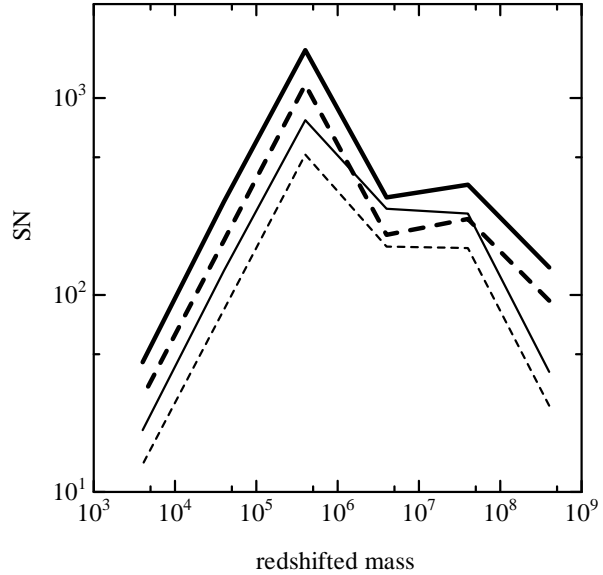


FIG. 1: Averaged SNR for equal mass binaries at $z = 3$. The thick curves are for TDI method and thin ones for method by Cutler. The results for the single (double) image is given by dashed (solid) curves respectively. The horizontal axis represents the redshifted mass m_z .

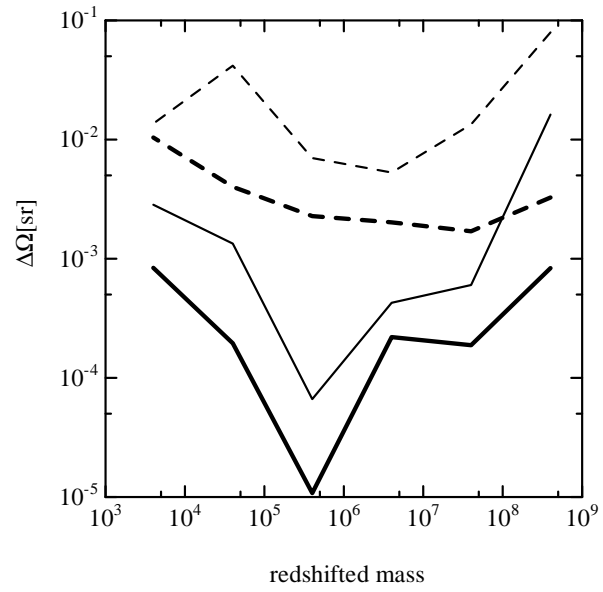


FIG. 2: Averaged angular resolution. Captions for curves are same as figure 1.

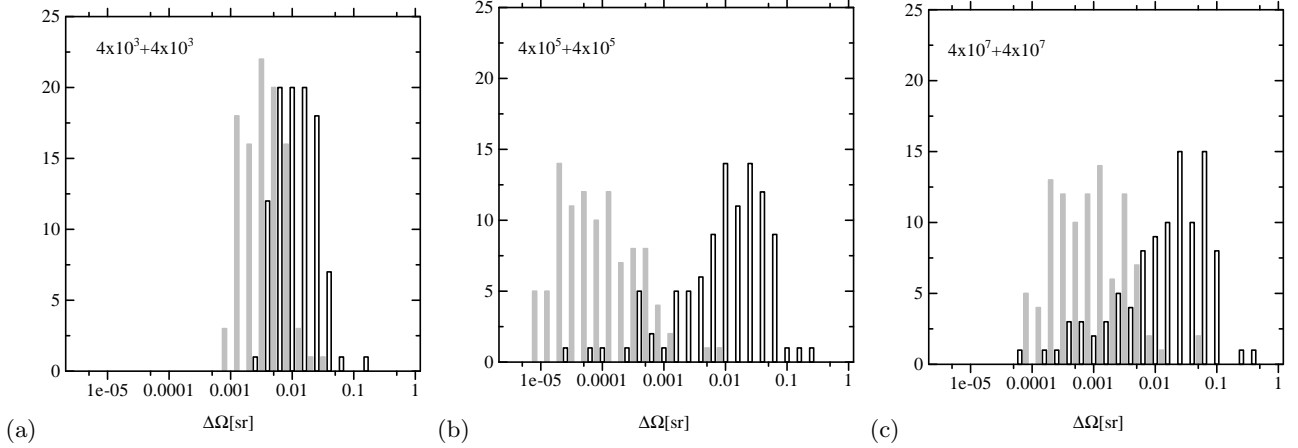


FIG. 3: Histograms of the angular resolution $\Delta\Omega_1$ (open bars) and $\Delta\Omega_2$ (gray bars). The mass m_z is fixed at (a) $m_z = 4 \times 10^3$, (b) 4×10^5 and (c) 4×10^7 . The results for $\Delta\Omega_1$ are displaced by $10^{-0.1}$. Total number of bins is 100 for each mass. TDI method is used.

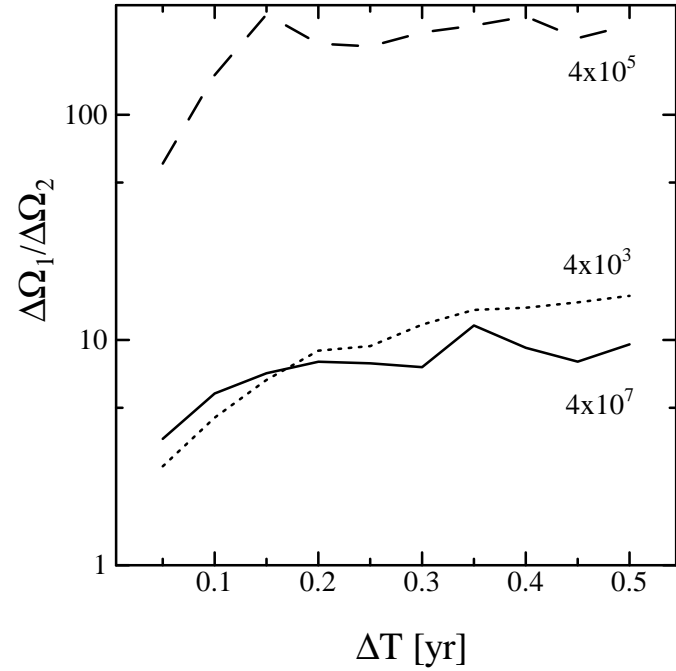


FIG. 4: Averaged ratio $\Delta\Omega_1/\Delta\Omega_2$ as a function of the time delay ΔT . Three curves are given for different masses. These results do not depend on the distances to the binaries. TDI method is used.

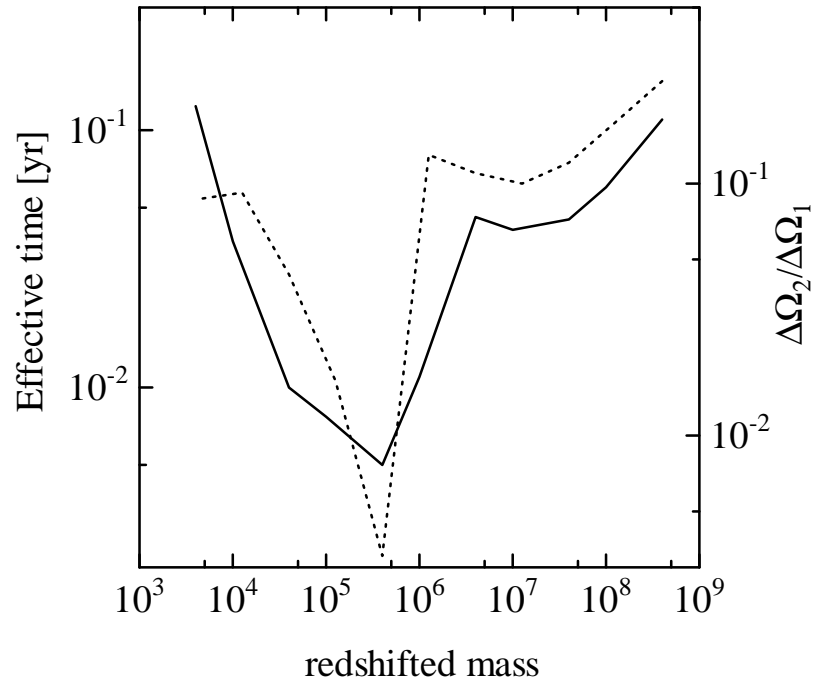


FIG. 5: The effective time t_{eff} (solid curve: left axis) and the ratio $(\Delta\Omega_1/\Delta\Omega_2)^{-1}$ (dotted curve: right axis) as functions of the redshifted mass m_z . TDI method is used.